Unprecedented Raman cascading and four-wave mixing from second-harmonic generation in optical fiber

Vincent Couderc,* Alessandro Tonello, Christelle Buy-Lesvigne, Philippe Leproux, and Ludovic Grossard

XLIM Research Institute-UMR CNRS 6172, Faculté des Sciences et Techniques, Université de Limoges, 87060 Limoges, France

**Corresponding author: vincent.couderc@xlim.fr*

Received September 4, 2009; revised November 24, 2009; accepted November 26, 2009; posted December 9, 2009 (Doc. ID 116707); published January 12, 2010

We experimentally demonstrate strong second-harmonic-generation from a self-induced all-optical poling in germanium-doped fiber with a subnanosecond laser pump at 1064 nm. The large second-harmonic conversion efficiency allows nonlinear spectral broadening at visible wavelengths so that up to nine distinct Raman sidebands have been obtained. In this work we emphasize how the Raman scattering, induced from the pump in the IR region, can drastically affect the optical poling effect, limiting in turn second-harmonic generation. © 2010 Optical Society of America

OCIS codes: 190.2620, 190.4370, 190.5650.

Second-harmonic generation (SHG) is generally not permitted in conventional silica fibers: The second-order nonlinear response vanishes in silica glasses, owing to their intrinsic molecular centro-symmetry. However inhomogeneities located at the core-cladding interface as well as electric-quadrupole and magnetic-dipole moments can concur to create an effective second-order nonlinear response. Other mechanisms can also improve the efficiency of the SHG in fibers. Since the pioneering work of Terhune *et al.* in bulk calcite, sum-frequency generation (SFG) has been obtained in germanium-doped fiber [1]. Österberg and Margulis [2] and Stolen and Tom [3] showed that second-order nonlinear effects in fiber could be significantly enhanced with an optical poling method. In this technique, the beating between a fundamental wave and its second harmonic is exploited to induce a longitudinally modulated static electric field. The resulting spatial displacement of local charges can create an equivalent periodic poling greatly enhancing the quasi-phase-matching condition. The quasi-phase-matched SHG was exploited as a pump source for a dye laser in [4]. Complementary studies on SHG coherence, phase measurement, SHG in multimode fibers, and photoinduced SHG in rare-earth doped fibers have also been reported [5–8]. To emphasize the second-order nonlinearity in fibers, several other poling techniques have been proposed and developed [9,10]. Tunable quasi-phase matching has been demonstrated in fiber by applying a strain force along the entire periodic structure. Although SHG in silica fiber has been largely investigated in the past, the relatively low conversion efficiency has always prevented from developing further applications. In particular, to our knowledge, no study on the direct implication of SHG energy in large spectral broadening has been published yet. Only the role of cross-phase modulation between fundamental and second-harmonic waves has been investigated in germanium-doped microstructured fiber [11].

In this work, we show how the SHG obtained in Ge-doped fiber, which is monomode in the IR region, can give birth to a large spectral broadening in the visible spectrum. Indeed the obtained second-order nonlinear conversion efficiency is large enough to induce Raman cascading and four-wave mixing (FWM) effects in the visible spectrum. We also experimentally identified the Raman scattering phenomenon as one of the main limitations of the optical poling process itself. Moreover, by using a circularly polarized pump, the optical poling induces a helical grating, and hence the SHG is made polarization independent.

The laser source delivers subnanosecond pulses (870 ps) at a repetition rate of 30 kHz. The output beam is circularly polarized because of the laser structure. The maximum peak power, which is really coupled into the fiber, Corning standard Ge-doped (3 mol. %) single-mode HI 980, is nearby 19 kW (500 mW of average power). The mode-field diameter at 1064 nm is 4.2 μm, and the propagation losses are below 2.5 dB/km at 980 nm. We use a CCD camera, a spectrum analyzer, and a fast photodiode to study the spatial, spectral, and temporal profiles of the output field.

When using the maximum available injected peak power (19 kW), the output spectrum largely broadens between 1060 and 1800 nm [Fig. 1(a)]. The main mechanism is the Raman cascading in normal dispersion. Three Stokes waves are generated at 1118, 1177, and 1243 nm. Beyond the zero-dispersion wavelength at 1.3 μm, modulation instability, soliton propagations, fission, and Raman frequency shift all contribute to generate a wide infrared spectrum. The output spectrum characteristics depend on the optical poling exposure time, i.e., the migration of the local charges. For short exposure time (less than 60 s) no SHG and no visible light have ever been observed. After 15 min of exposure time, a green radiation at 532 nm is clearly detected. This power continuously

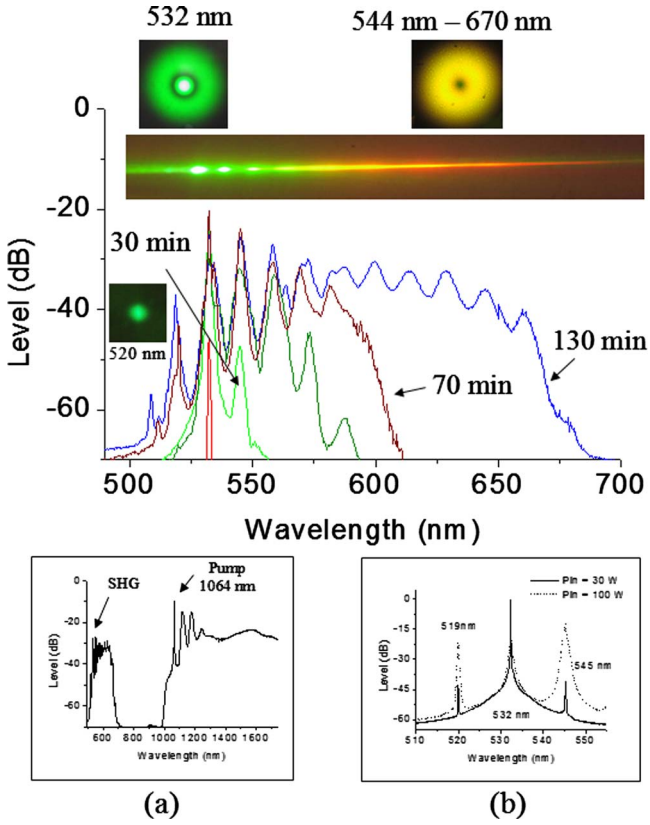

Fig. 1. (Color online) Visible spectral evolution induced by the converted wave at the second harmonic versus writing time (input peak power at 1064 nm: 19 kW; fiber length, 20 m) and with output far field patterns. (a) Visible and IR spectra; (b) visible spectrum generated from a single 532 nm input pump (fiber length, 20 m).

grows thanks to the action of the self-optical-poling of the silica Ge-doped fiber and propagates on the fundamental transverse mode. This effect, largely reported elsewhere [3–8], is explained by the progressive displacement of local charges. Here the IR pump is not linearly polarized as in other cases previously reported in the literature but exhibits circular polarization state; consequently, polarization insensitive quasi-phase matching is obtained. Hence the generated harmonic wave is also circularly polarized. After 30 min of exposure time, a second sharp peak is obtained at 545 nm, which could correspond to a Raman sideband from the converted SHG at 532 nm and/or to the SFG between the pump radiation at 1064 nm and its first Stokes wave at 1118 nm. For longer exposure time, a second and then a third Stokes sideband are obtained in the SHG spectrum. This observation confirms our interpretation of the Raman cascading process. After more than 2 h of exposure, nine Stokes waves have been clearly observed in the visible domain at the fiber output. At this step the second-harmonic wave propagates on a combination of several LP_{02} modes, whereas the Raman Stokes waves exhibit a ring shape also constituted by linear superimposition of LP_{11} modes. Finally, blue-green radiations located at 508 and 520 nm are also observed propagating on the fundamental LP_{01} mode (Fig. 1). These radiations are located at the Raman anti-Stokes wavelengths, but surprisingly their powers are too large to be generated by the Raman process alone. Additionally, no phase matching is obtained with any other visible wavelengths, suggesting that the usual phase-matched FWM is not involved in this phenomenon. Actually, Raman anti-Stokes radiations may be amplified through the FWM mediated coupling with Raman Stokes waves under non-phase-matched conditions, as already predicted and observed in [12]. This assumption is supported by the fact that our experiments fulfill the criterion mentioned in that paper, i.e., $|\Delta k| \gg |2\gamma q P_P|$, where $\Delta k = 2k_{P,\mathrm{LP02}} - k_{S,\mathrm{LP11}} - k_{\mathrm{AS,LP01}}$ is the linear phase mismatch, γ is the fiber nonlinearity coefficient, $|q| \sim 0.86$, and P_P is the launched pump peak power [in our case, $\gamma = 2\pi n_2/(\lambda A_{\mathrm{eff}}) \sim 29\ \mathrm{W^{-1}\ km^{-1}}$ calculated with $n_2 = 3.2 \times 10^{-20}\ \mathrm{m^2/W}$ and $A_{\mathrm{eff}} \sim 13\ \mu\mathrm{m}^2$, leading to $|\Delta k|/|2\gamma q P_P| \sim 200$]. Besides the initial step of the SHG, no significant further influence of the IR spectrum to the visible spectrum is observed. To confirm this fact we have also pumped the same type of fiber directly with a subnanosecond radiation at 532 nm [Fig. 1(b)]. The obtained visible spectrum shows the same qualitative features as those obtained when the 532 nm line is created by the SHG of a laser pump at 1064 nm in the first few tens of centimeters of the fiber. These observations tend to confirm that the spectral broadening in the visible region originates from the SHG of the pump power, in the absence of any significant influence of further energy conversion from the wideband infrared radiation which is created in parallel. The visible spectrum obtained from the SHG in fiber covers more than 160 nm between 508 and 677 nm (Fig. 1). The corresponding SHG conversion efficiency, taking into account the fiber losses, is 3.5% (7%) of the input IR average (peak) power and all the generated wavelengths in the IR and visible regions exhibit circular polarization. No photodegradation of the fiber, which could be due to the relatively high green peak power propagating in the Ge-doped silica core, is observed over 3 h of the operation.

In a second set of experiments, we have recorded the IR and visible spectral broadening at different positions in the fiber by using the cut-back technique (see Fig. 2). This operation allows us to distinguish the characteristic lengths of the different nonlinear phenomena. For each fiber length we measured the spectrum shape, the output powers at 532 and at 1064 nm, and the temporal profiles of the IR and visible waves. The input pump power was kept fixed to its maximum level of 19 kW (peak power). For the first 45 cm no spectral broadening of the IR or visible waves was detectable, except for a narrowband SHG signal. Beyond a half of 1 m of the fiber, a significant Raman process is observed in the infrared domain, which in turn drastically depletes the pump at 1064 nm. At the same time, the SHG power saturates, and its related Raman cascading line becomes clearly evident in the visible domain (Fig. 2).

Thanks to the cut-back procedure we are able to show both the IR pump (1064 nm) and the SHG (532 nm) powers upon the fiber length (Fig. 3). We can

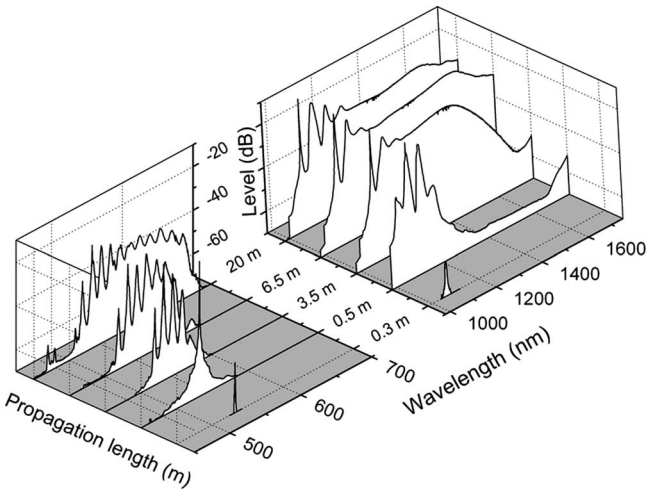

Fig. 2. Visible and IR spectrum evolutions versus fiber length after poling process (input IR peak power at 1064 nm: 19 kW; writing time, 130 min).

clearly see that after a few meters, the 1064 nm radiation is drastically depleted and it reaches its minimum value of 20 mW at a distance of 20 m. This rapid consumption of the IR pump represents the major limitation to the writing process of the longitudinal nonlinear grating, which is the real engine of the SHG efficiency. We can conclude that the SHG is principally generated within the first few meters of the fiber. These results agree also with those of [2], where a limitation of the SHG along the optical fiber after just a half of meter of propagation and for 20 kW of the IR pump power is shown. To our knowledge, nobody has identified yet the limitation induced into the optical poling process, and then the ultimate limits to the SHG efficiency in the fiber. Only an explanation of the SHG saturation due to phase modulation between the fundamental and the second harmonic writing beams was discussed [6].

Beyond the spectral analysis, evidence of optical poling breakdown induced by the stimulated Raman process can also be recorded in the temporal domain. Indeed, a large pump depletion is observed, whereas the first Raman Stokes wave at 1118 nm grows larger with a poor temporal overlap between the pump and

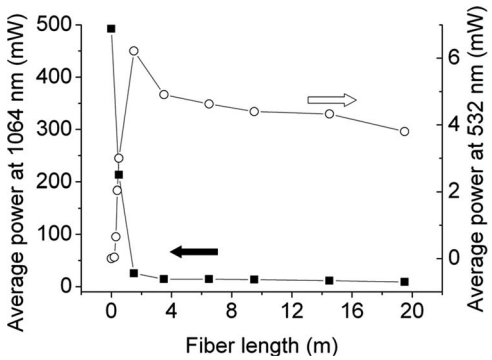

Fig. 3. Output power evolution versus fiber length. Circles, 532 nm; squares, 1064 nm.

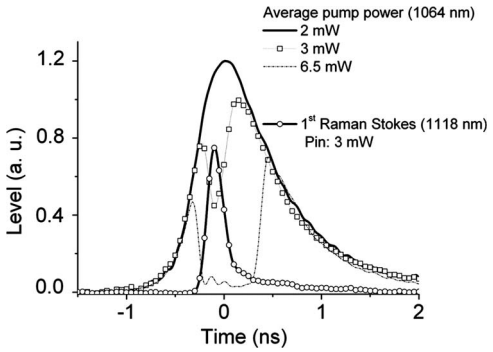

Fig. 4. Output pulse shape at 1064 and 1118 nm versus input pump power (fiber length, 20 m; writing time, 130 min).

the visible radiations. This low temporal superimposition limits the beating between the fundamental wave and its second harmonic and stops the poling process. In the same manner a weak temporal overlap between the Stokes pulse at 1118 nm and the remaining depleted pump at 1064 nm is obtained limiting the SFG in the visible domain (Fig. 4). Therefore the main mechanism of the spectral broadening in the visible domain definitely is the Raman process.

We have reported a large SHG in a Ge-doped silica fiber whose nonlinear response was previously conditioned by an all-optical poling obtained from a circularly polarized IR pump. The conversion efficiency at 532 nm can be strong enough to broaden significantly the spectrum in the visible domain through FWM and Raman processes. Nine distinct Raman Stokes sidebands have been observed in the visible spectral domain. We have also identified the IR Raman scattering as the main limiting factor for the optical poling contributing to the SHG.

References

1. R. W. Terhune, P. D. Maker, and C. M. Savage, Phys. Rev. Lett. **8**, 404 (1962).
2. U. Österberg and W. Margulis, Opt. Lett. **12**, 57 (1987).
3. R. H. Stolen and H. W. K. Tom, Opt. Lett. **12**, 585 (1987).
4. U. Österberg and W. Margulis, Opt. Lett. **11**, 516 (1986).
5. B. Ehrlich-Holl, D. M. Krol, R. H. Stolen, and H. W. K. Tom, Opt. Lett. **17**, 396 (1992).
6. W. Margulis, I. C. S. Carvalho, and J. P. von der Weid, Opt. Lett. **14**, 700 (1989).
7. M. A. Saifi and M. J. Andrejco, Opt. Lett. **13**, 773 (1988).
8. E. M. Dianov, L. S. Kornienko, A. O. Rybaltovsky, P. V. Chernov, and Y. P. Yatsenko, Opt. Lett. **19**, 439 (1994).
9. P. G. Kazansky, L. Dong, and P. St. J. Russell, Opt. Lett. **19**, 701 (1994).
10. A. Canagasabey, C. Corbari, Z. Zhang, P. G. Kazansky, and M. Ibsen, Opt. Lett. **32**, 1863 (2007).
11. V. Tombelaine, C. Buy-Lesvigne, P. Leproux, V. Couderc, and G. Mélin, Opt. Lett. **33**, 2011 (2008).
12. S. Coen, D. A. Wardle, and J. D. Harvey, Phys. Rev. Lett. **89**, 273901 (2002).